ELSEVIER

Modelling and optimisation of solid electrolyte sintering behaviour by thermokinetic analysis

A.C. Müller [a,*], J.R. Opfermann [b], E. Ivers-Tiffée [a]

[a] *Institut für Werkstoffe der Elektrotechnik, Universität Karlsruhe (TH), Adenauerring 20, D-76131 Karlsruhe, Germany*
[b] *NETZSCH Gerätebau, Wittelsbacherstr. 42, D-95100 Selb, Germany*

Abstract

Burnout of organic binder and sintering behaviour of yttria doped zirconia electrolyte green tapes were investigated by thermogravimetry and dilatometry. The burnout which precedes the actual sintering, as well as the sintering itself were described by a mathematical model based on formal kinetics. Thus, the measured data were reduced to a set of a few parameters which can be easily used to simulate the kinetic behaviour for an arbitrary temperature profile, so that good accordance between prediction and respective measurement was accomplished. Using rate controlled binder burnout and rate controlled sintering, optimisation of the temperature profile was achieved with respect to time and energy saving. These results were confirmed by SEM analysis of the microstructure and determination of the electrical conductivity.
© 2003 Elsevier B.V. All rights reserved.

1. Introduction

Due to the increasing demand for energy worldwide and the resulting impact on the environment, new alternative methods of energy production have to be developed. Solid oxide fuel cells (SOFC) are a promising candidate as they can directly convert the chemical energy stored in hydrogen or natural gas into electrical energy with high efficiency at elevated temperatures of 973–1273 K [1–3]. To increase performance and long term stability and to decrease production costs, a lot of research has been and is being done to look for alternative materials and production techniques. In this paper, attention was focused on the sintering optimisation of electrolytes which are made by tape casting, and often used as the supporting element in SOFCs.

Usually a fine ceramic powder is mixed with an organic binder, and tape casting is used to form a green body. In a subsequent process, the binder is removed by a thermal treatment, and the green body is sintered at high temperatures to build a dense ceramic.

Most properties of ceramics, like density, mechanical stability and electrical conductivity, strongly depend on the temperature profile used for sintering. As the electrolyte should have a high density ≥98% to be gas tight, low heating rates and high temperatures are preferable, but these conditions are in discordance with industrial applications. A reasonable way to fulfil both requirements—high density and a fast temperature profile—was introduced by Palmour [4,5] and is better known as rate controlled sintering (RCS).

Usually the transducer signal of a push-rod dilatometer is used to adjust the temperature profile (heating rate) in such a way that a constant shrinkage rate can be achieved. However, it would be desirable to describe the sintering behaviour with the help of a thermokinetic model, because in that way the shrinkage curve for an arbitrary temperature profile can be easily calculated and optimised by computer without resorting to further experiments. It can be especially useful for the evaluation of temperature profiles to cofire different materials. However, it would be nearly impossible to apply a scientific model which describes the individual steps of sintering by physical/chemical processes, because

---
* Corresponding author. Tel.: +49-7216087569; fax: +49-7216087492.
E-mail addresses: axel.mueller@iwe.uni-karlsruhe.de (A.C. Müller),
j.opfermann@ngb.netzsch.com (J.R. Opfermann),
ellen.ivers-tiffee@iwe.uni-karlsruhe.de (E. Ivers-Tiffée).
URLs: http://www.iwe.uni-karlsruhe.de, http://www.netzsch.com,
http://www.iwe.uni-karlsruhe.de.

this is quite complex [7–9]. Therefore, another approach was used in this work.

A kinetic model based on a simple but in principle arbitrary mathematical model that reduces the measured data to a set of a few formal parameters was used. In the case of isothermal sintering, there are some phenomenological formulas which describe the sintering behaviour and which proved their value [10]. But as we are interested in dynamic temperature profiles, sintering experiments with different heating rates were carried out in a push-rod dilatometer and analysed with an advanced thermokinetic software tool [11,12]. Having used a combination of several reaction steps which were based on the technique of formal kinetics, a comprehensive model was built up. Different reaction types were used and their dependence on temperature was described by an Arrhenius term. The parameters of the model were obtained by multivariate nonlinear regression because single curve regressions often lead to incorrect results as indicated in [12,13]. Further details of the basic concepts of the software package can be found in [13]. The application of the software tool to sintering behaviour of ceramic bulks was first introduced in [14,15]. In the present work, this method was applied to examine the sintering behaviour of thin green tapes whereby isothermal segments were incorporated into the evaluation.

Besides the applied sintering profile, the temperature profile used for burnout of the organic binder has a great impact on the sintering behaviour of the green bodies. Therefore the binder burnout of the samples was first analysed by the use of thermogravimetry (TG) and later evaluated by the above-mentioned thermokinetic software package. From the analysis of the data, a temperature profile for rate controlled mass loss (RCM) was evaluated and applied before the actual sintering.

The electrical conductivity of differently sintered specimens was determined and their microstructure was analysed by electron microscopy. Based on these results, an optimal temperature profile for binder burnout and sintering was selected.

2. Experimental

2.1. Burnout of organic binder

Zirconia green tapes with different types of dopant were investigated: 8 mol% yttria (8YSZ), 8 mol% yttria with 1 mol% alumina (8Y1ASZ) and 3 mol% yttria (3YSZ). The specimens had a thickness of about 200 μm (8YSZ, 8Y1ASZ) and 70 μm (3YSZ). Details concerning the composition of the organic binder and the tape processing are unknown as the samples were obtained from a company. For the determination of the binder burnout kinetics, samples of about 25 mg were heated up from room temperature to 873 K in a NETZSCH TG209 thermogravimetric microbalance at heating rates of 2, 5 and 10 K/min. A constant air flow rate of 100 ml/min was used to remove the organic burnout.

The relative length change due to the sintering shrinkage was measured in air in a NETZSCH DIL402C push-rod dilatometer. To prevent the samples from adhering to the measurement system, thin alumina disks were positioned on both sides of the sample. Influences caused by the measurement setup were corrected by previous calibration measurements with a 1 mm thick alumina disk (99.9%) under the same conditions as the specimen.

For the determination of the influence of the binder burnout on sintering behaviour, samples were heated up to 573 K in the dilatometer using different burnout profiles. Afterwards, a constant heating rate of 5 K/min up to 1473 K was applied.

2.2. Sintering behaviour

For the actual sintering experiments, the temperature profiles were divided into three segments. For the first segment—the binder burnout—an optimised RCM temperature profile obtained from the evaluation of the former thermogravimetric measurements was used. Afterwards, the samples were fired to 1673 K at different heating rates of 2, 5 and 10 K/min and then they were held at this temperature for 2–5 h.

The microstructure of the samples after binder burnout and sintering was analysed in a Leo Gemini 1530 electron microscope. The electrical conductivity of the sintered specimen was determined in the temperature range of 573–1223 K in air by four-point dc measurements.

Thermokinetic analysis of the binder burnout and sintering were carried out with the help of the *Thermokinetics* software from NETZSCH [11].

3. Results and discussion

3.1. Burnout of organic binder

In Fig. 1, TG curves (symbols) for the mass change of the 8Y1ASZ samples during binder burnout are presented. For the TG curve with a heating rate of 2 K/min, binder burnout began at 383 K and ended at 643 K. For higher heating rates, onset and end of burnout were shifted to higher temperatures. The overall mass loss of about 18% was the same for all heating rates, as was expected. Derivation of the mass loss curves with respect to time (Fig. 2) revealed that the burnout process was subdivided into four single steps. As the individual mass losses of the single steps were independent of the heating rate, a kinetic model with four consecutive steps was chosen (for a graphical representation, see Fig. 1). For every single step, a reaction type of *n*th order was used [11,13]. Nonlinear multivariate regression was carried out to adjust the model parameters to the measured data. The parameters obtained are given in Table 1. The
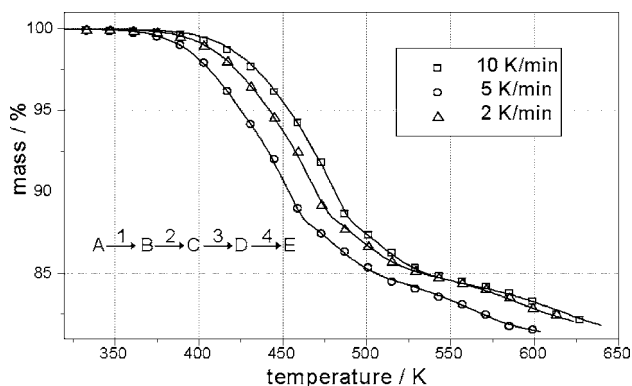
Fig. 1. TG curves of the 8Y1ASZ binder burnout were carried out at different heating rates. A four-step model was used for the simulation (symbols: measurement, lines: simulation).
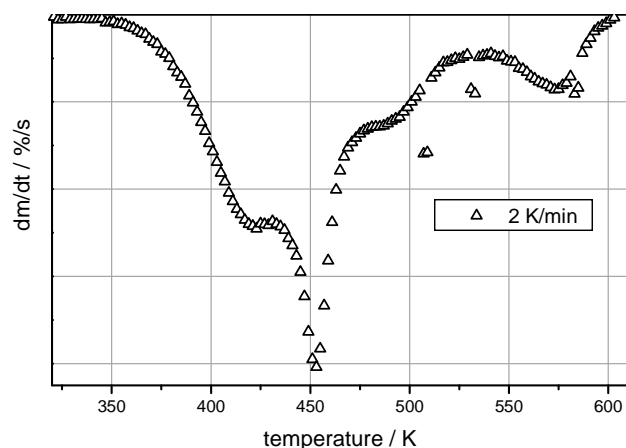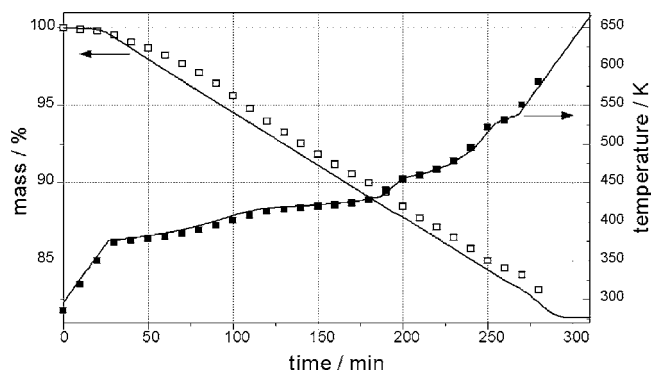

Fig. 3. Comparison between prediction (lines) and measurement (symbols) of 8Y1ASZ green tapes mass loss due to binder burnout for an RCM temperature profile (0.07%/min).

Fig. 2. Derivation of the TG curve of 8Y1ASZ with a heating rate of 2 K/min. Four peaks can be identified.

simulated curves which resulted from these parameters are shown in Fig. 1 as solid lines and are in good accordance with the measured data (correlation coefficient of 0.9994). Because of the reduction of the kinetic data to a set of a few formal parameters, it is now possible to easily calculate the mass loss for an arbitrary temperature profile. Therefore, the applied model and its parameters were verified by calculating a temperature profile for a rate controlled mass loss of 0.07%/min (RCM-007) and by comparing it with an actual

measurement based on this temperature profile. The heating rate was limited to a range from 0.1 to 3 K/min. As shown in Fig. 3, the accordance of prediction and measurement is excellent. Thus, the proposed model is adequate to describe the binder burnout. But it should be remembered that the model is only a formal description of the binder burnout process, and that physical or chemical interpretation of the kinetic parameters should not be over-stated. Furthermore it should be emphasised that the parameters obtained are valid only for the type of specimen examined here. If one uses, for example, a different thickness or particle size distribution, the results will be altered.

To obtain the optimal burnout profile, the microstructure of samples exposed to different burnout profiles was analysed by SEM and the influence on the sintering behaviour was determined by dilatometry. SEM analysis indicated that high heating rates were accompanied by large pores and cracks due to the fast evaporation of the organic binder. However, a uniform microstructure is important for an early sintering onset and high final density after sintering [16]. Both the samples treated by a low constant heating rate of 2 K/min (CHRM-2) and the RCM samples revealed a homogeneous microstructure. However, great differences were visible in their sintering behaviour. In Table 2, sintering onset and total shrinkage between sintering onset and 1473 K are given for various burnout profiles.

It is obvious that sintering of the RCM samples began at lower temperatures in comparison with the CHRM samples. Furthermore, it can be seen that the energy-conservative RCM profiles also lead to higher shrinkage in the same

Table 1
Kinetic parameters of the four-step model describing the binder burnout of 8Y1ASZ green tapes

Parameter	Value	Parameter	Value	Parameter	Value
$\log(A1/s^{-1})$	6.8	$\log(A3/s^{-1})$	9.5	Foll reaction 1	0.3
$E1$ (kJ/mol)	75.4	$E3$ (kJ/mol)	113.0	Foll reaction 2	0.3
Reaction order 1	1.0	Reaction order 3	1.4	Foll reaction 3	0.2
$\log(A2/s^{-1})$	9.1	$\log(A4/s^{-1})$	4.3	Mass loss 1/%	−18.1
$E2$ (kJ/mol)	101.8	$E4$ (kJ/mol)	78.3	Mass loss 2/%	−18.1
Reaction order 2	0.5	Reaction order 4	0.9	Mass loss 3/%	−18.1

For the meaning of the parameters, see [13].

Table 2
Influence of different binder burnout profiles on sintering behaviour of 8Y1ASZ

Burnout profile	Burnout time (min)	Sintering onset (K)	Shrinkage at 1473 K (%)
1 K/min (CHRM-1)	285	1282	6.7
0.1%/min (RCM-01)	210	1279	7.4
0.07%/min (RCM-007)	285	1275	7.3

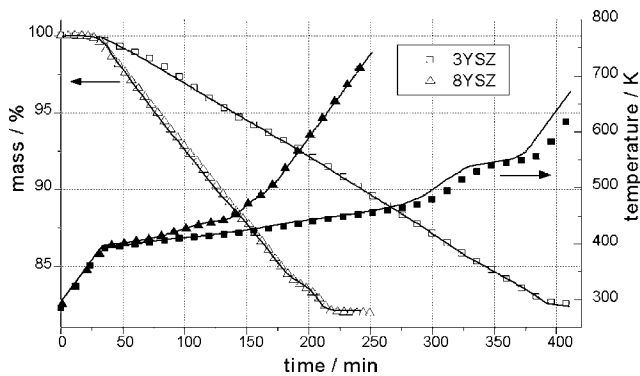After binder burnout (573 K), the samples were fired at 5 K/min to 1473 K.

Fig. 4. Comparison between prediction (lines) and measurement (symbols) of 8YSZ (0.1%/min) and 3YSZ (0.05%/min) green tapes mass loss due to binder burnout for an RCM temperature profile.

Fig. 6. Sintering behaviour of 8Y1ASZ green tapes for different heating rates as a function of time. The sintering onset is set to time null for better representation. A four-step model was used for the simulation (symbols: measurement, lines: simulation).

(RCM-007) or in even less time (RCM-01). It is assumed that the different sintering behaviour is caused by small deviations in particle contacts which influence the diffusion processes during sintering and which cannot be resolved by SEM.

Similar thermogravimetry investigations were carried out with the 8YSZ and 3YSZ specimens. For both types of samples, the same kinetic model was chosen as for the 8Y1ASZ specimen. The model parameters calculated were of course different. The excellent accordance between prediction and measured data is shown in Fig. 4. For the 3YSZ specimen, an RCM profile with a mass loss of 0.05%/min was chosen, because analysis of the microstructure by SEM indicated large pores for higher rates due to the small thickness of these specimens as can be seen in Fig. 5. Based on these results, the RCM profiles listed in Table 3 were selected for the subsequent sintering investigations.

3.2. Sintering behaviour

The sintering curves obtained by dilatometry were divided into three segments. In the first segment, the organic binder was burnt out according to the RCM profiles which were evaluated in the last paragraph. Only a small length change occurred in this segment. Between the end of the binder burnout and the sintering onset, the samples indicated a positive length change of about 3% which can be ascribed to thermal expansion and to a slight bending of the samples due to their small thickness. The actual shrinkage curves of the 8Y1ASZ specimen are presented in Fig. 6. For better illustration, only the sintering regime is shown and sintering onset of the different curves was set to time null. Sintering onset occured between 1251 and 1275 K and was shifted to higher temperatures for higher heating rates. Most of the shrinkage occurred during the dynamic heating, whereby the samples in the isothermal segment shrunk by only about 1%. Values for sintering onset and shrinkage are given in Table 4. Densification of all samples was completed after the isothermal segment.

For the thermokinetic modelling, a four-step model was used as indicated in Fig. 6. As proposed by Opfermann et al. [14,15], the sintering process can be formally described by two consecutive reactions (nth order and diffusion type) which are followed by two competing reactions (Avrami–Erofeev type [11] and nth order). Two

Table 3
RCM profiles selected for the subsequent sintering investigations

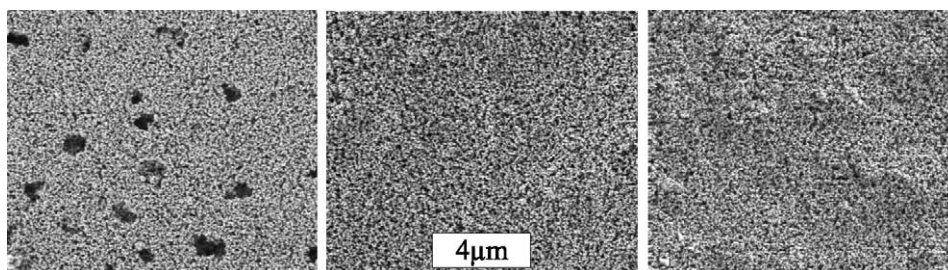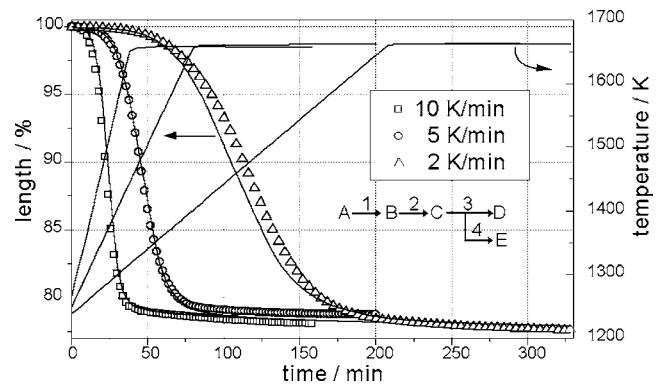| Sample	Mass loss rate (profile)
8Y1ASZ	0.1%/min (RCM-01)
8YSZ	0.1%/min (RCM-01)
3YSZ	0.05%/min (RCM-005)

Fig. 5. SEM images of the 3YSZ tapes after binder burnout. Left: 5 K/min; mid: 2 K/min; right: 0.05%/min.

Table 4

Dependence of sintering onset and total shrinkage on heating rate of the 8Y1ASZ specimen

Heating rate (K/min)	Sintering onset (K)	Shrinkage at 1673 K (%)	Total shrinkage
2	1251	21.6	22.3
5	1258	20.6	21.3
10	1275	20.7	21.9

competing steps are absolutely necessary, because the total shrinkage depends on the heating rate, as shown in Table 4 and in Fig. 6. This behaviour is well known from sintering theory [7]. Multiple processes like surface, volume and grain boundary diffusion take place simultaneously. A diffusion reaction type was used for the second reaction because a better fit could be achieved than for the *n*th order reaction type used in [14,15]. The results of the nonlinear multivariate regression are shown in Fig. 6 as solid lines. The multivariate regression yielded a correlation coefficient of 0.998. The model parameters used are given in Table 5. One can see that the contribution of the first two reaction steps to the overall shrinkage is small. They determine the sintering onset.

Based on this model and its parameters, an RCS temperature profile was calculated and an appropriate measurement was carried out. Comparison between prediction and actual measurement is shown in Fig. 7 and indicates a good agreement. Thus, the applied model and its parameters can be seen as valid to describe the sintering behaviour.

Comparable results were obtained for the 3YSZ and 8YSZ. A four-step model with two competitive reactions was also applied and the model parameters were determined by nonlinear multivariate regression. With the help of these parameters, temperature profiles for a constant shrinkage rate (RCS) were calculated. As shown in Figs. 8 and 9, a good accordance between prediction and actual measurement was achieved. After incorporation of the RCS measurements in the model, a further enhancement of the final regression was achieved.

With the help of the thermokinetic models, optimal temperature profiles for sintering were calculated for all types of specimen in compliance with the following constraints:

- maximum shrinkage for dense electrolyte;
- in best time;
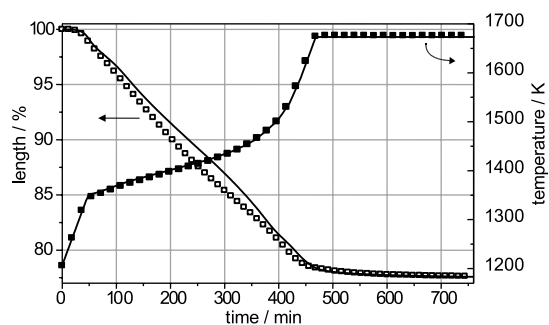- lowest possible final temperature;

Fig. 7. Comparison between prediction (lines) and measurement (symbols) of 8Y1ASZ green tapes sintering behaviour for an RCS temperature profile (0.05%/min).
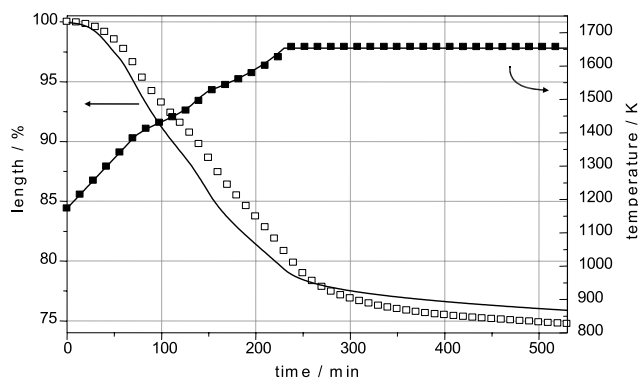

Fig. 8. Comparison between prediction (solid lines) and measurement (symbols) of 8YSZ green tape sintering behaviour for an RCS temperature profile (0.5%/min).
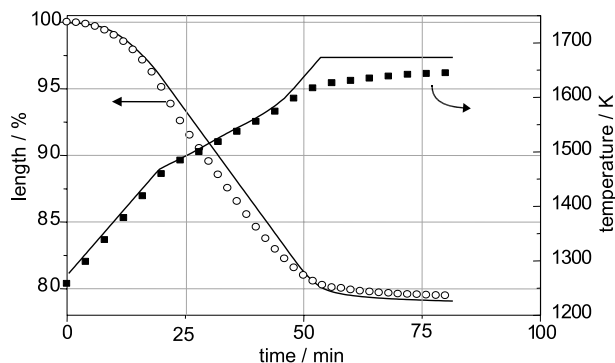

Fig. 9. Comparison between prediction (solid lines) and measurement of 3YSZ green tape sintering behaviour for an RCS temperature profile (0.1%/min).

Table 5

Kinetic parameters of the four-step model used to describe the sintering behaviour of 8Y1ASZ green tapes. For the meaning of the parameters see [13]

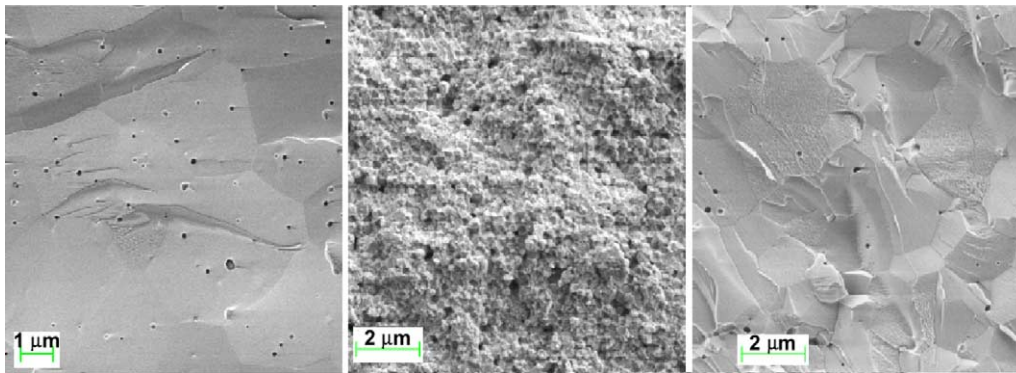| Parameter	Value	Parameter	Value	Parameter	Value
$\log(A1/\text{s}^{-1})$	16.60	$\log(A3/\text{s}^{-1})$	7.45	Reaction order 4	2.89
$E1$ (kJ/mol)	527.42	$E3$ (kJ/mol)	420.56	Foll reaction 1	0.08
Reaction order 1	1.77	Dimension 3	0.41	Foll reaction 2	0.06
$\log(A2/\text{s}^{-1})$	16.77	$\log(A4/\text{s}^{-1})$	24.59	Competitive reaction3	1.00
$E2$ (kJ/mol)	570.34	$E4$ (kJ/mol)	788.67	Competitive reaction4	0.07

Fig. 10. Microstructure of 8Y1ASZ (left), 3YSZ (mid) and 8YSZ (right) specimen sintered with an RCS profile.

Table 6
Optimised sintering profiles

Sample	Shrinkage rate (%/min)	Final temperature (K)	Holding time (h)	Total time (h)
8Y1ASZ	0.05	1673	3	27.5
8YSZ	0.1	1623	5	25.7
3YSZ	0.1	1653	5	26.2

- maximum heating rate of 3 K/min;
- minimum heating rate of 0.1 K/min.

Priority was set according to this list.

The optimal profiles for the various sample types are given in Table 6. Thus, the total sintering time for electrolyte tapes—including binder burnout and cooling down—was reduced to less than 28 h, and a decrease of the final sintering temperature was also possible. This results in a saving of time and energy.

All samples exhibited a homogeneous and dense microstructure (Fig. 10) and the final grain size distribution was narrower in comparison with samples sintered at a constant heating rate, due to the uniform grain growth during sintering. This is in accordance with the results obtained by Palmour et al.[4] and Abe and Yamada[6]. No differences
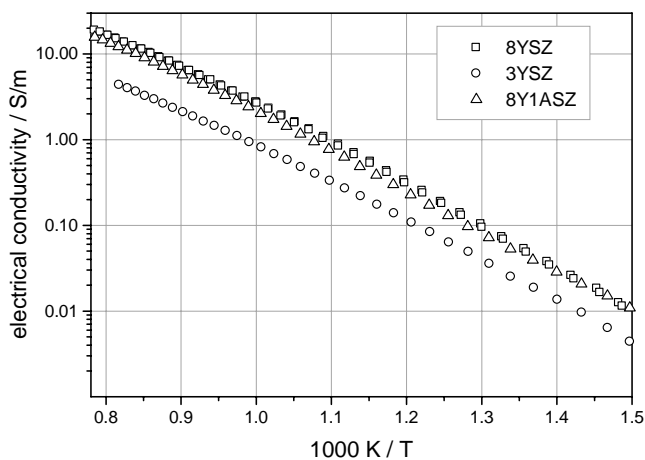
in electrical conductivity were detected in comparison with samples sintered at a constant heating rate and all samples had values comparable with the data given in the literature [17–20], as can be seen in Fig. 11.

4. Conclusions

The burnout of the organic binder and the sintering behaviour of electrolyte green tapes based on zirconia were investigated by means of thermokinetic analysis. It was shown that the binder burnout which precedes the actual sintering, as well as the sintering itself, can be described by a mathematical model based on formal kinetics. By multivariate regression, the measured data were reduced to a set of a few parameters which were used to easily simulate the kinetic behaviour for an arbitrary temperature profile without knowledge of the physical nature of the underlying processes.

For the binder burnout, a model with four single consecutive steps was chosen and validated by comparison between prediction and respective measurement. Using a temperature profile for a constant mass loss rate, a positive influence on the sintering behaviour is observed. Sintering onset was decreased and shrinkage increased in comparison with a conventional constant heating rate profile.

The sintering behaviour was described by a four-step model with two competing reactions which led to a good accordance between prediction and measurement. Based on this model, temperature profiles for rate controlled sintering were evaluated. SEM analysis of the microstructure and determination of the electrical conductivity as a function of temperature revealed that by using rate controlled binder burnout and rate controlled sintering, optimisation of the temperature profile can be achieved with regard to time and energy saving.

Fig. 11. Electrical conductivity of 8Y1ASZ, 8YSZ and 3YSZ specimen sintered with an RCS profile.

References

[1] N.Q. Minh, J. Am. Ceram. Soc. 76 (3) (1993) 563–588.
[2] E. Ivers-Tiffée, W. Wersing, H. Greiner, Ceramic components for a SOFC with metallic interconnector, in: R. Waser (Ed.), Electroce-

ramics IV: Electroceramics and Applications I–III, Augustinus Buch-
handlung, Aachen, 1994, pp. 719–724.

[3] E. Ivers-Tiffée, A. Weber, D. Herbstritt, J. Europ. Ceram. Soc. 21
(2001) 1805–1812.

[4] H. Palmour III, M.L. Huckabee, T.M. Hare, Rate controlled Sinter-
ing: Principles and Practice, in: M.M. Ristic (Ed.), Sintering—New
Developments, Elsevier, Amsterdam, 1979, pp. 46–56.

[5] H. Palmour III, T.M. Hare, in: G.C. Kuczynski, D.P. Uskokovic, H.
Palmour III, M.M. Ristic (Eds.), Sintering'85, Plenum Press, New
York, 1987, p. 17.

[6] O. Abe, J. Yamada, J. Ceram. Soc. Jpn. 102 (1994) 627–631.

[7] Ja.E. Geguzin, Physik des Sinterns, Deutscher Verlag für Grund-
stoffindustrie, Leipzig, 1973.

[8] Y. Moriyoshi, W. Komatsu, Yogyo-Kyokai-Shi 79(10) (10) (1971)
370–375.

[9] J. Frenkel, J. Phys. (USSR) 9 (1945) 385.

[10] U.A. Ivensen, Zeitschrift für technische Physik (russ.) (1947).

[11] J. Opfermann, NETZSCH Thermokinetics 2, Version 2003.09, NET-
ZSCH Gerätebau GmbH.

[12] A.K. Burnham, Thermochim. Acta 355 (2000) 165–170.

[13] J. Opfermann, J. Therm. Anal. Cal 60 (2000) 641–658.

[14] J. Opfermann, J. Blumm, W.-D. Emmerich, Thermochim. Acta 318
(1998) 213–220.

[15] J. Blumm, J. Opfermann, U. Janosovits, H.-J. Pohlmann, High
Temperatures-High Pressures 32 (5) (2000) 567–572.

[16] T. Fang, H. Palmour III, Ceram. Int. 16 (1990) 63–71.

[17] M. Mori, M. Yoshikawa, H. Itoh, T. Abe, J. Am. Ceram. Soc. 77 (8)
(1994) 2217–2219.

[18] M. Mori, T. Abe, H. Itoh, O. Yamamoto, Y. Takeda, T. Kawahara,
Solid State Ionics 74 (3–4) (1994) 157–164.

[19] V.V. Kharton, E.N. Naumovich, A.A. Vecher, J. Solid State Elec-
trochem. 3 (1999) 61–81.

[20] S.P.S. Badwal, J. Mater. Sci. 19 (1984) 1767–1776.